P1.3   DIURNAL VARIABILITY OF THE CLOUD FIELD OVER THE VOCALS DOMAIN FROM GOES IMAGERY

José M. Gálvez[1], Raquel K. Orozco[1], and Michael W. Douglas[2]

[1] CIMMS/University of Oklahoma, Norman, OK 73069
[2] NSSL/NOAA, Norman, OK 73069

1. INTRODUCTION

As part of ongoing studies of mesoscale variability over the South American altiplano, we produced averages of the cloudiness using GOES imagery. These composites, made at full resolution of the imagery, helped to identify the relationship between the underlying topography and the cloud field. Having in mind that one of the objectives of the upcoming VOCALS activity is to describe the diurnal variability of the stratocumulus over the southeastern Pacific and their relationship to the South American continent, we have produced GOES imagery composites for this region. The frequent absence of clouds in the middle and upper troposphere makes satellite observations an excellent tool to describe the stratocumulus variability in this region of the world.

The study is carried out over a rectangular domain located between 1°N, 19°S, 68.5°W and 96.5°W, which covers the tropical southeastern Pacific ocean including the Peruvian and Ecuadorian coasts. The dataset is based on 30-minute temporal resolution and 4km horizontal resolution visible and IR4 GOES-8 imagery for an entire year starting on May 2002. The results are stratified per time of the year and cloud-top temperature frequency thresholds, and are organized to describe the diurnal and seasonal variation of the cloudiness and its apparent propagation offshore. Comparison is made with the simulated diurnal cycles reported in the literature.

2. BACKGROUND

Subtropical marine stratocumulus regimes occur all over the world in regions of high static stability associated to semi-permanent high pressure systems. These include the Peruvian (SE Pacific), Namibian (SE Atlantic), Californian (NE Pacific), Australian (SE Indian) and Canarian (NE Atlantic) regimes, all located in the eastern ends of a subtropical oceanic region (Klein and Hartmann, 1993). These types of regimes are believed to play a key role in the coupled atmospheric-ocean processes that determine the local and remote sea surface temperature (SST) and related climate interactions by modifying the radiative balance (Ma et. al, 1996; Xu et. al. 2005). Ma et. al. (1996) found using a GCM that the Peruvian stratocumulus exert a strong influence on the climate in regions away from the Peruvian coast such as the equatorial Pacific as far west as the dateline. Philander (1996) found that the feedback provided by stratocumulus is crucial in producing realistic meridional asymmetries in the eastern Pacific. Nigam (1996), based on a study carried out in the Eastern Equatorial Pacific, proposed a positive feedback mechanism

in which radiative cooling from the stratocumulus tops generates southerly surface winds, which in turn foster stratocumulus growth from the increased meridional cold advection and latent heat flux.

The variability of the Peruvian marine stratocumulus regime has also been explored in previous studies. Seasonal analyses describe a cloud frequency maximum during the cold season and a minimum during the warm season (Stowe et. al., 1989; Klein and Hartmann, 1993; Norris, 1997). The peak stratocumulus cloud amount occurs between September and November with nearly 72% of the region covered, and the minimum occurs between December and March with a coverage of 42% according to Klein and Hartmann (1993). Norris (1997) showed similar results with a the cold season maximum located offshore from the Peruvian coast at 12-18°S and 80-82°W, and the warm season maximum west from the Chilean coast at 22-28°S and 78-80°W.

3. METHODOLOGY

The database utilized consists on 30-minute 4-km resolution GOES-8 visible and infrared channel 4 (IR4) images for an entire year starting on May 2002. The domain selected is a sector of the tropical southeastern Pacific Ocean cropped to domain located from 1°N to 19°S and from 68.5°W to 96.5°W (figure 1). Two techniques are applied for the cloudiness analysis: Pixel averaging and pixel frequency calculations. Since the major goal of the study is to describe and compare the diurnal cycle of the stratocumulus, the techniques are applied in an hourly basis leading to several hourly composites per analysis.

The pixel averaging technique was applied only to the visible imagery. Frequency calculations were only suitable for the IR4 channel since the visible channel is constrained by the strong diurnal cycle of the reflected solar radiation. Furthermore, a strong non-linear correlation between the IR4 channel radiance detected and the temperature of the emitting body allows the conversion of the goes counts into temperature, leading to the calculation of frequency analyses based on cloud top temperatures.

Seasonal changes are taken into account. For this, temporal stratifications in the order of 1-month, 3-month and 6-month periods are applied. The results here presented are summarized to describe the diurnal cycles corresponding to opposite seasons: the cool (i.e. June-November) and warm (i.e. December-May) season. For a spatial analysis, frequencies averaged over four 4°x4° selected sectors are compared (figure 1). The northeast sector (NE), centered at 8°S and 83°W, attempts to describe the diurnal and seasonal cycles of the stratocumulus offshore from the northern Peruvian coast. The southeast sector (SE), centered at 16°S and 80°W, is designed to describe the variability offshore from the southern Peruvian coast, one of the regions with the largest frequency of stratocumulus clouds especially during the cool season. The southwest (SW) and northwest (NW) sectors, centered at 16°S-90°W and 8°S-90°W respectively, are selected to describe the zonal variation of the stratocumulus clouds after compared to the SE and NE sectors.
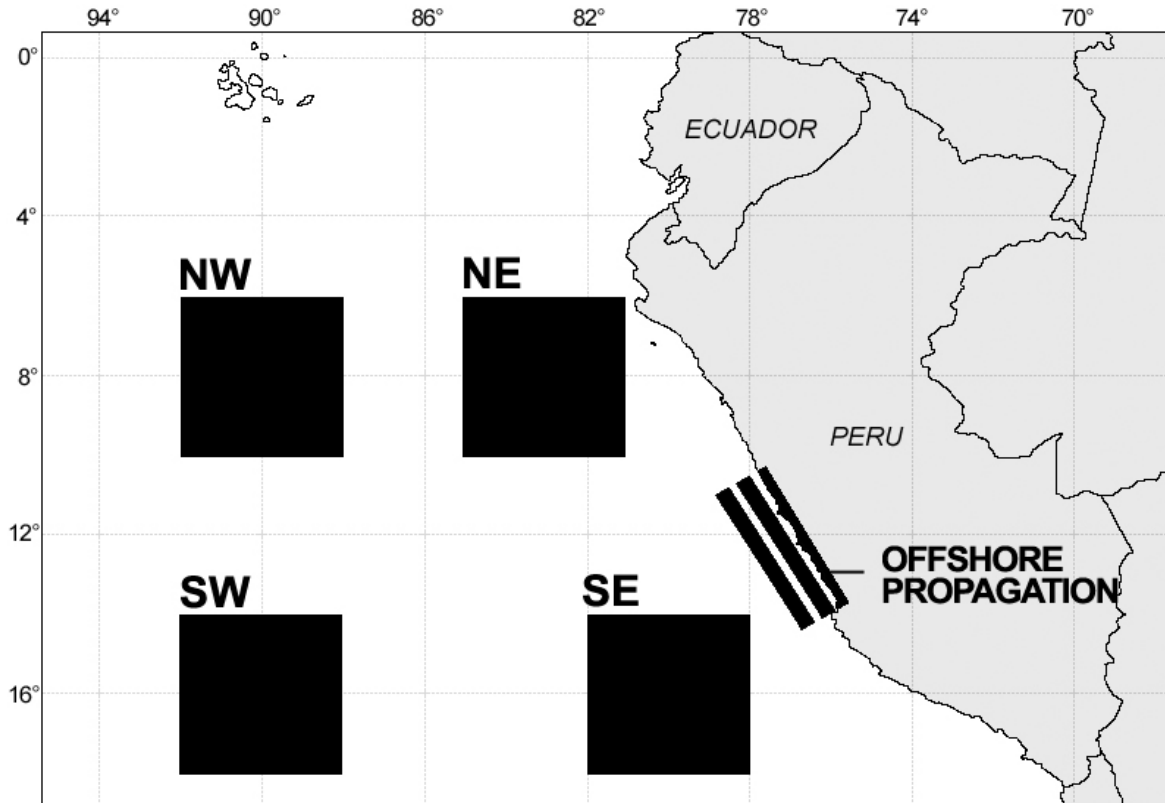
Fig. 1. Domain of study including the 4 square sectors selected for the description of the spatial distribution of the diurnal cycles and the three strips selected for the offshore propagation analyses.

The offshore propagation of the stratocumulus clouds was also discussed by comparing frequencies averaged over 3 narrow bands along and offshore from the central Peruvian coast. These 3 bands are also illustrated on figure 1.

4. RESULTS AND DISCUSSION

As expected, the diurnal and also the seasonal variability of the SE Pacific stratocumulus cloud field were evident from GOES-8 visible and infrared satellite imagery, and the results showed agreement with the simulated diurnal cycles reported on the literature. According to the satellite composites, the stratocumulus clouds appear to be more frequent and more widespread during the night than during the day and during the cool season in contrast to the warm one.

Figures 2 and 3 show the visible images for the morning (09:15 LST Peru) and afternoon (14:45 LST Peru) averaged over the cool and warm seasons respectively. They suggest that during the cool season the marine stratocumulus are the most persistent and widespread, in particular during the mornings, with the regions of the maximum brightness located (1) near and over the coast at 0.5-2.5°S, 10.5-13.5°S and 16-19°S, and (2) over a region offshore from central and southern Peru located at 12-17°S and 78-82°W. By the afternoon, a brightness decrease observed from figure 2a to figure 2b suggests partial and periodic dissipation over the entire domain. The regions of maximum dissipation occur over certain areas in the Peruvian coast and immediately offshore.

Likewise, during the warm season the stratocumulus clouds are more frequent during the morning than during the afternoon hours. In this case, however, lower brightness over the entire ocean when compared to the corresponding cool season brightness suggests less cloudiness during this period. This is true especially north of 14° and along the Peruvian coast, which agrees with the stratocumulus climatology presented by Norris (1998). The diurnal variations during the summer also suggest that the clouds decrease towards the afternoon over the entire ocean with the exception of the equatorial Pacific where the diurnal cycle is not that apparent. Solar reflection over a region located between 4° and 8° S and west of 86°W leads to larger values of brightness and therefore complicates the analysis over this area.

In order to compare the two opposite phases of the stratocumulus diurnal cycle, cloud top temperature frequency analyses are presented in figure 4. The frequency of cloud tops cooler than 12.5°C calculated for the cold season is displayed for 01:45 LST Peru (during the night) and for 13:45 LST (during the early afternoon). The continent is shaded in solid black.

Frequency calculations should be analyzed carefully since they do not necessarily provide information about the presence of the stratocumulus but do give information regarding how often the stratocumulus tops become high enough to cool down below the temperature threshold used. Larger frequencies observed during the night than during the day over the entire domain reveal indirectly a diurnal cycle of the cloud height, indicating deeper clouds during the night as opposed to shallower clouds during the afternoon. A southeast-northwest frequency gradient indicates that the deepest stratocumulus develop offshore from the southern Peruvian coast, whereas shallower and warmer convection describe the equatorial region. These frequency analyses are calculated only over the cool season so the effects of the deeper convection associated to the rarely present double ITCZ are disregarded since this feature forms around the month of March.

Seasonal and geographical variations of the diurnal cycle

Seasonal and geographical variations of the diurnal cycle were also explored and summarized in figure 5 using frequency calculations. Eight curves corresponding to the diurnal cycle of cloud top temperatures below 12.5° is presented for the four the SE, SW, NE and NW sectors described in figure 1. The analysis has been stratified for the cold and warm seasons.

Overall, the frequencies peak 2 hours after local midnight (07 UTC) but remain almost constant throughout a 7-hour period confined between 05 and 12 UTC. Dissipation processes associated to solar radiation, which peak between 13 and 19 UTC, place the lowest cloud frequencies in the early afternoon, between 17 and 22 UTC. The amplitude of the diurnal cycle is maximized near the coast where the effects of the diurnally heated continent contribute to a much rapid dissipation of the morning clouds.
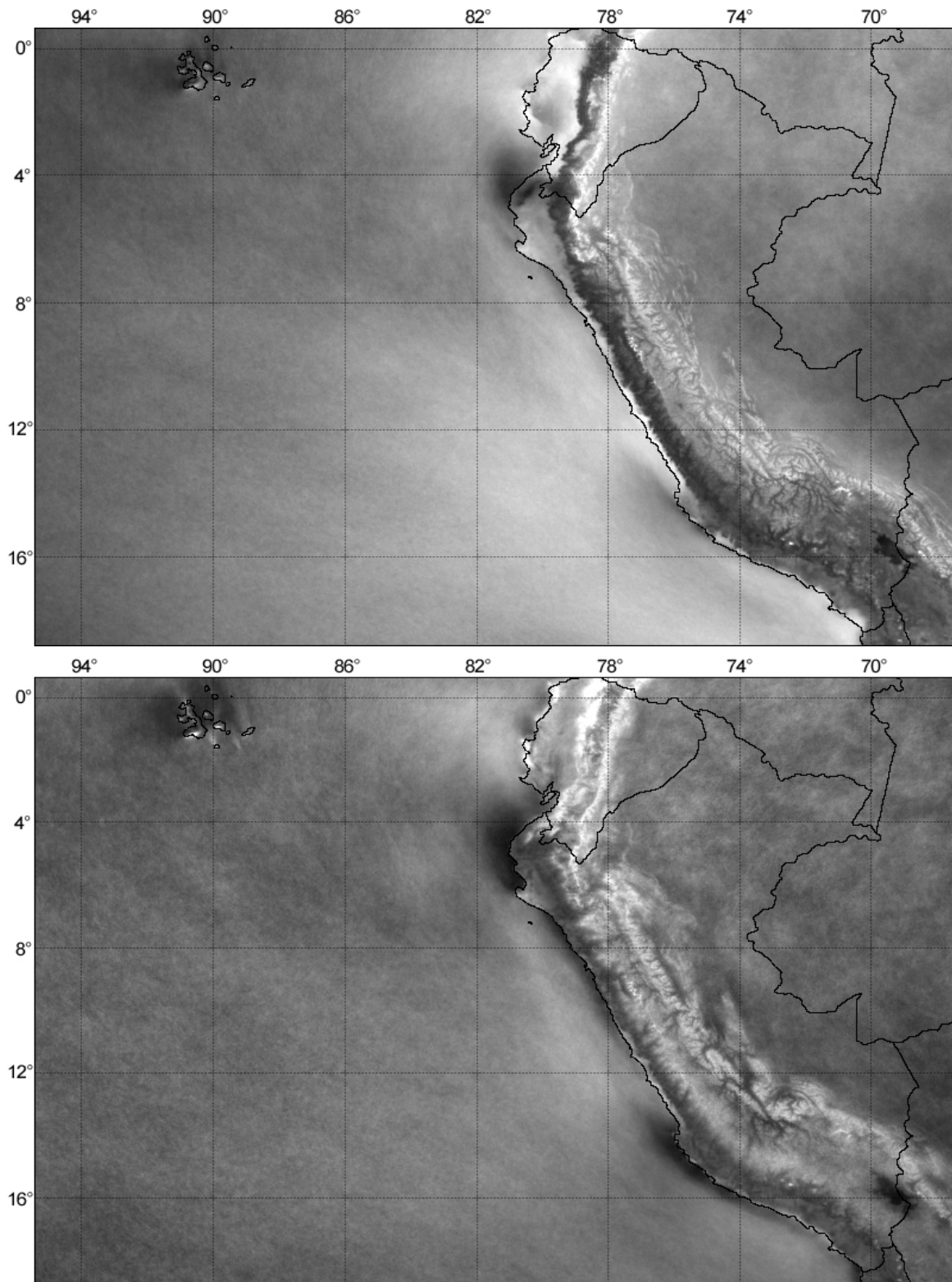
Fig. 2. Morning (top) and afternoon (bottom) cloudiness composites based on daily GOES visible images averaged over the June–November 2002 (i.e. cold season). The images used to construct the top panel were captured at 14:15 UTC (9:15 LST Peru) and the ones for the bottom panel at 19:45 UTC (14:45 LST Peru).
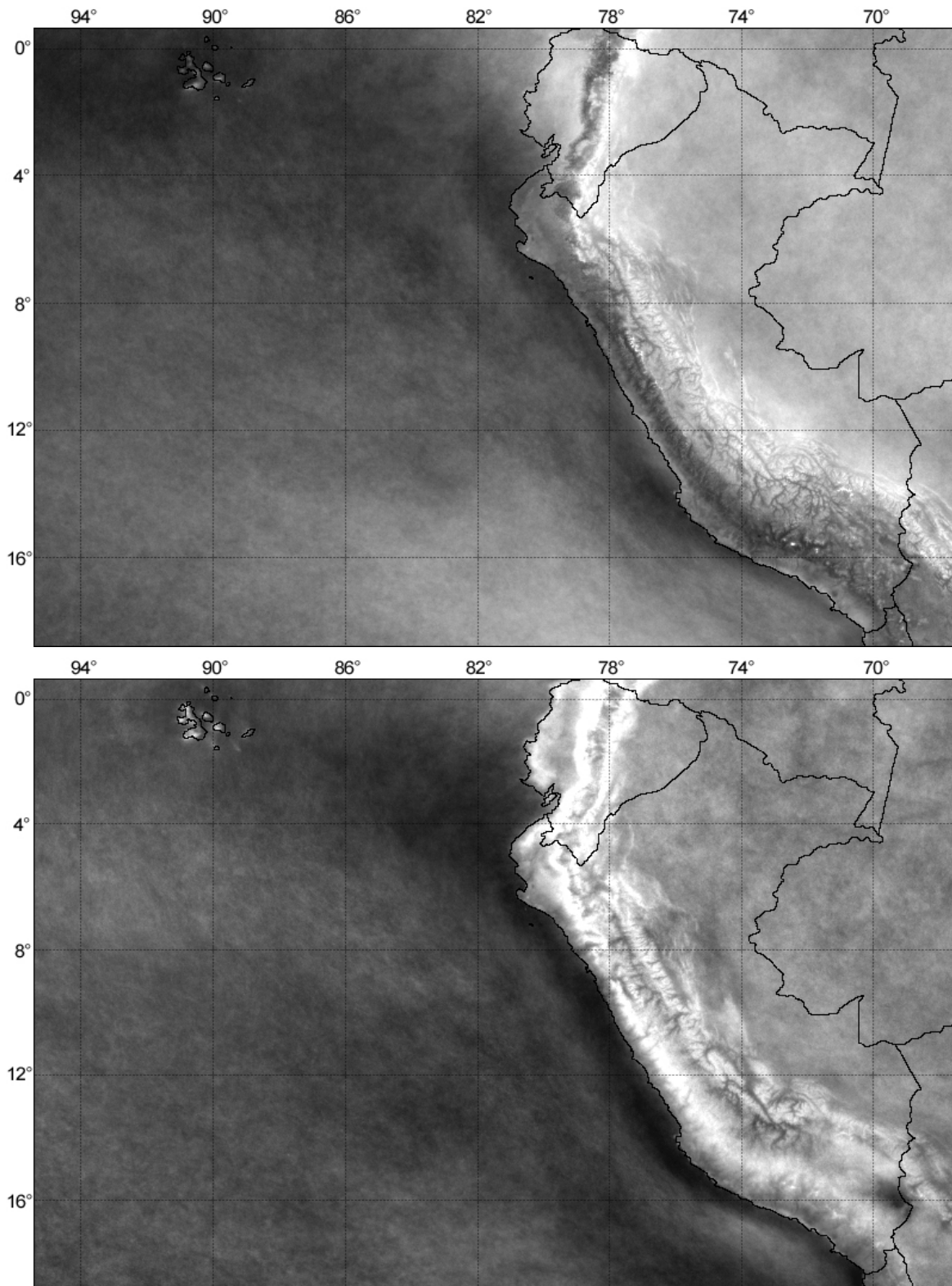
Fig. 3. Morning (top) and afternoon (bottom) cloudiness composites based on daily GOES visible images averaged over the December–May 2002-3 (i.e. warm season) period. The images used to construct the top panel were captured at 14:15 UTC (9:15 LST Peru) and the ones for the bottom panel at 19:45 UTC (14:45 LST Peru), similarly to figure 1.
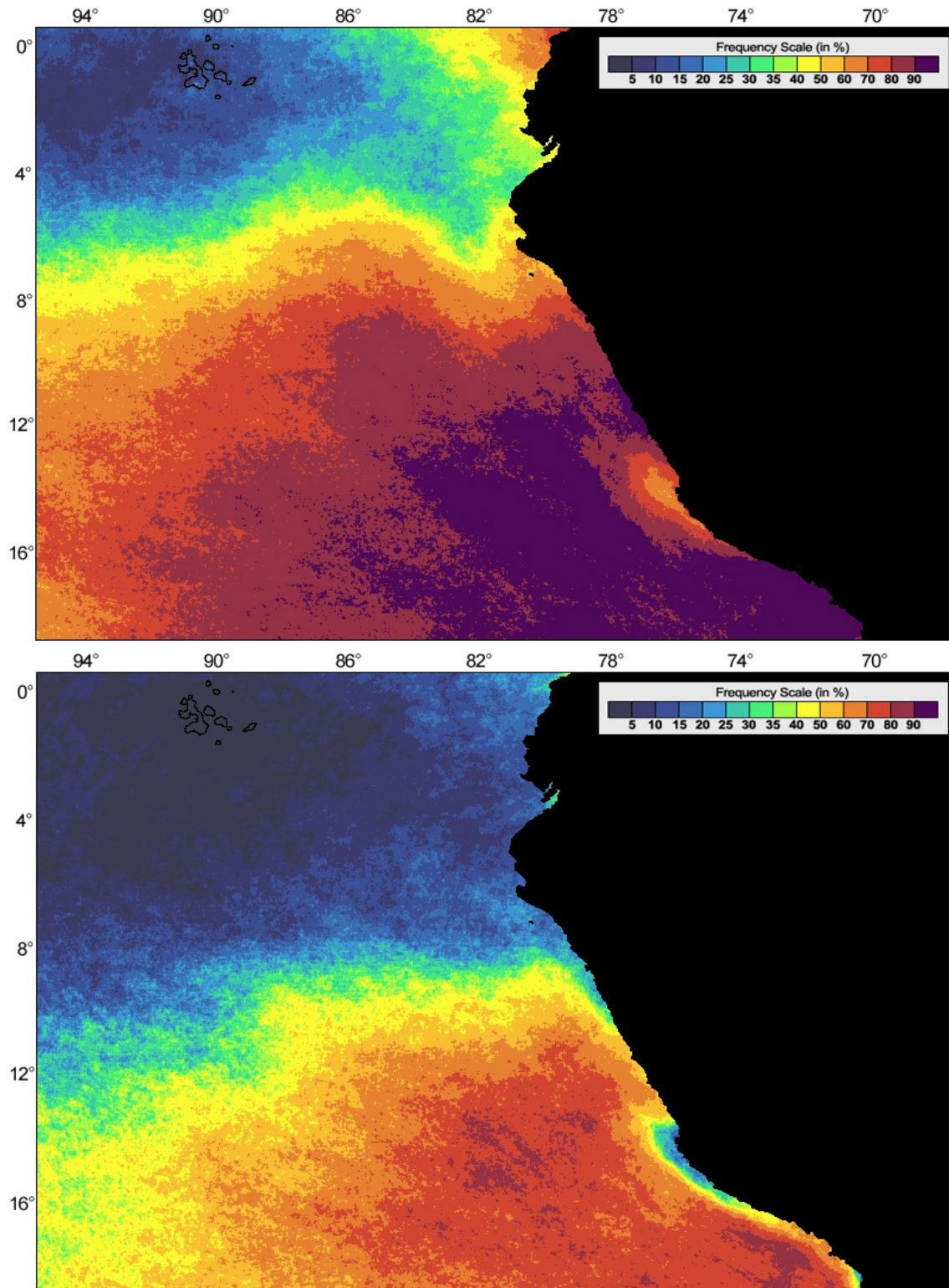
Fig. 4. Morning (top) and afternoon (bottom) frequency of clouds colder than 12.5° based on daily GOES IR4 images averaged over the June–November 2002-3 (i.e. cool season) period. The images used to construct the top panel were captured at 14:15 UTC (9:15 LST Peru) and the ones for the bottom panel at 19:45 UTC (14:45 LST Peru), similarly to figure 1.

The diurnal cycle of cloudiness is, in general, more pronounced during the summer than during the winter, especially at 16°S, according to the visible composite brightness field. The cloud temperature frequency analyses displayed in figure 5 are coherent with these findings. They imply that the amplitude of the diurnal cycle of clouds colder than 12.5°C is larger during the summer than during the winter, indicating that both the amount of clouds and cloud depth vary. At 8°S, however, the frequency analysis indicates that the diurnal variability is more ample during the winter, which implies a larger change in the depth of the clouds than on the presence of the stratocumulus.

Figures 2, 3 and 5, in agreement with the literature, also suggest that the seasonal variability is more pronounced immediately offshore from the South American coast than at 90°W, especially during the day when cloud free skies are frequent near the continent in the afternoons. While the SW sector's frequency oscillates between 50 and 80% during the cool season, and the cloudier SE sector's frequency between 75 and 95%, during the warm season the diurnal cycle of frequency is comparable for both the regions and oscillates between 20 and 65%.
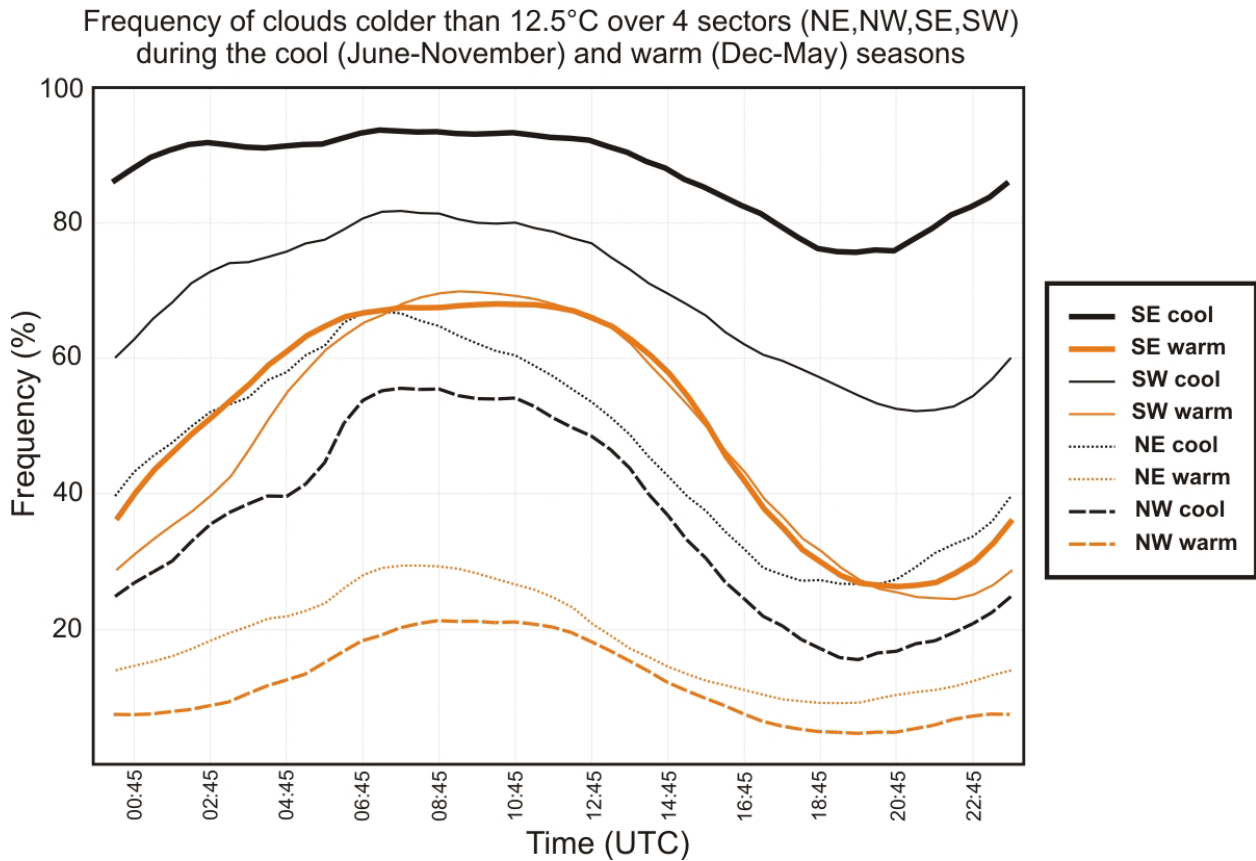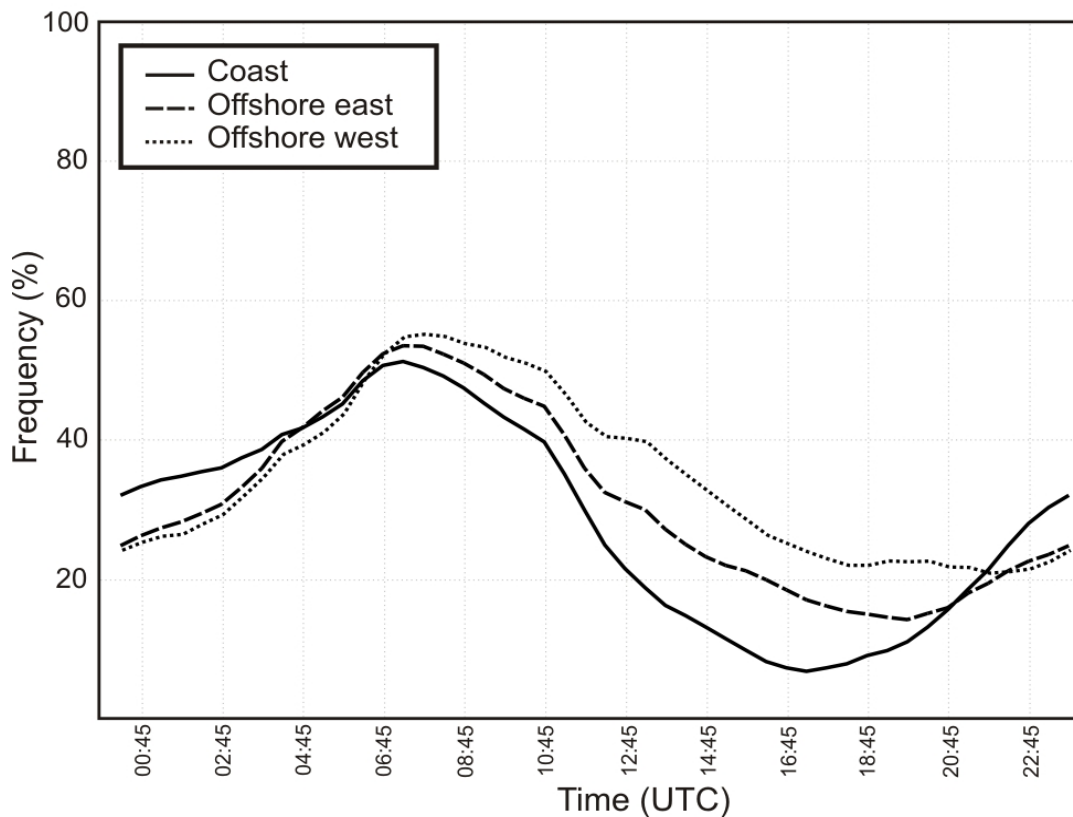

Fig. 5. Diurnal cycle of the frequency of clouds colder than 12.5°C, averaged over 4 different sectors off the Peruvian coast and stratified by season. The sectors are the 4° x 4° squares presented on figure 1. The SE sector (thick solid lines) is centered at 16°S and 80°W; the SW sector (thin solid lines) is centered at 16°S and 90°W; the NE sector (dotted line) is centered at 8°S and 83°W and the NW sector (dashed line) is centered at 8°S and 90°W. Black curves correspond to the cool season (June through November) and orange curves to the warm season (December through May).

Regarding the length of cloudy and cloud-free periods, the findings suggest that the "cloudy" nocturnal regime prevails over the less cloudy diurnal regime at 16°S whereas at 8°S the contrasting regimes are balanced in time.

Westward propagation off the coast of South America

The offshore propagation of the stratocumulus clouds during the cool season is explored. The frequency of clouds colder than 10°C is averaged over three sectors aligned with the central Peru's coastline (see figure 1) during the cold season, and the hourly averages are presented in figure 6. Indeed, the results suggest that the clouds originate/dissipate first over the Peruvian coast and propagate towards the west. From 21:45 UTC (16:45 LST) through 04:15 UTC (11:15 LST) the largest frequencies of stratocumulus clouds occur over the coast and the lowest away from it. This relationship reverses between 07:45 UTC (02:15 LST), right after the frequency peaks over all the regions, and 20:45 UTC (15:45 LST).

Fig. 6. Diurnal cycle of the frequency of clouds colder than 10°C at 3 sectors along the central Peruvian coast during the cool season (June through November). The sectors are indicated in figure 1. The coastal one covers the Peruvian coast from 10°S through 14°S and about 40 inland from the Pacific Ocean. The east offshore sector consists on a 60km fringe offshore and along the coastal sector. The west offshore sector covers a similar fringe just west of sector 1.

The hour of maximum cloud frequency occurs very close in time in the three regions with a lag of about 30 minutes from the coast and the western offshore sector and the largest frequencies are in the order of 50-55% for all the regions. The coastal peak occurs about two hours after midnight, at 07:15 UTC or 02:15 Peruvian LST. In contrast, the hour of minimum stratocumulus coverage exhibits a lag of 5 hours starting over the coast at 17:15 UTC (12:15 LST), and the difference in the order of magnitude of the frequency is larger with <10% over the coast and >20% over the western offshore sector. The amplitude of the diurnal cycle of frequency is more pronounced over the coast than over the ocean in response to the diurnal heating of the low-lying terrain, which contributes to the dissipation of the clouds.

Westward propagation/migration over the open ocean is also apparent on the results from the large square sectors. Structures observed on the diurnal cycle corresponding to the western sector lag 1-2 hours the same ones observed over the eastern corresponding sectors.

5. CONCLUDING REMARKS

The stratocumulus diurnal cycles revealed by the GOES-8 visible and infrared satellite composites were in agreement with the ones described in the literature. The marine stratocumulus appear to be more frequent after midnight (i.e. cold cloud frequencies peak at 07 UTC) and during the morning than during the afternoon in response to the cloud-top radiative cooling, the main mechanism for their development, which peaks during the night. The seasonal cycle is also in agreement with the literature indicating larger cold cloud frequencies during the cool season versus shallower and less frequent clouds during the warm season, when the region of the largest cloudiness shifts southward into offshore northern Chile.

Spatial analysis of the diurnal cycle revealed that the cloudy nocturnal regime prevails over the less cloudy diurnal regime at 16°S whereas at 8°S the contrasting regimes are balanced in time. At 16°S the cloud depth and coverage diurnal cycle amplitude appears larger during the warm season than during the cold season, when cloudiness is more persistent. At 8°S the cloud coverage diurnal cycle amplitude does not vary much with the seasons but the cloud depth diurnal cycle amplitude is maximized during winter. Overall, the largest diurnal cycle was of cloudiness observed over the coast since the diurnally heated continent plays an additional role in the stratocumulus dissipation process. Offshore propagation with lags between 30 minutes and 5 hours were also observed.

The horizontal scale (~ 200 x 200 km) of the large stratocumulus clusters that develop offshore, when averaged over a 90-day period (i.e. ~70-80 images considering the missing ones), still produces some clustering noticeable on the 3-month composites. To eliminate this clustering and achieve a smoother description of the stratocumulus climatology, future work will concentrate on applying the same methodology over a longer dataset. This will increase the statistical significance of the analysis by increasing the number of degrees of freedom. Furthermore, a longer (3-year long or more) dataset may serve to filter the effects of low-frequency climate variations such as the El Niño Southern Oscillation (ENSO), which appears to have a large impact on the land-ocean-atmosphere system of western South America.

REFERENCES

Klein, S. A., and D. L. Hartmann, 1993: The seasonal cycle of low stratiform clouds. Journal of Climate, Vol 6, pp 1587-1606.

Ma, C., C. R. Mechoso, A. W. Robertson, and A. Arakawa, 1996: Peruvian Stratus Clouds and the Tropical Pacific Circulation: A Coupled Ocean-Armosphere GCM Study. Journal of Climate, Vol. 9, pp 1635-1645.

Nigam, S., 1997: The Annual Warm to Cold Phase Transition in the Eastern Equatorial Pacific: Diagnosis of the Role of Stratus Cloud-Top Cooling. Journal of Climate, Vol. 10, pp 2447-2467.

Norris, J. R., 1998: Low cloud type ofer the ocean from surface observations. Part II: Geographical and seasonal variations. Journal of Climate, Vol 11, pp 383-403.

Philander, S. G. H., D. Gu, D. Halpern, G. Lambert, N. C. Lau, T. Li, and R. C. Pacanowski, 2996a: The role of low-level stratus clouds in keeping the ITCZ mostly north of the equator. Journal of Climate, Vol. 9, in press.

Stowe, L. L., H. Y. M. Yeh, T. F. Eck, C. G. Wellemeyer, H. L. Kyle, 1989: Nimbus-7 Global Cloud Climatology. Part II: First Year Results. Journal of Climate, Vol 2, pp 671-709.

Xu, H., S. Xie and Y. Wang, 2005: Subseasonal variability of the southeast Pacific stratus deck. Journal of Climate, Vol. 18, pp 131-